Histol Histopathol (2023) 38: 1029-1041

Histology and Histopathology
From Cell Biology to Tissue Engineering

ORIGINAL ARTICLE Open Access

CircRNA PDE3B regulates tumorigenicity via the miR-136-5p/MAP3K2 axis of esophageal squamous cell carcinoma

Wei Yue, Yiwang Ye, Baokun Chen, Da Wu, He Wang and Gang Hui

Department of Thoracic Surgery, Peking University Shenzhen Hospital, Shenzhen City, Guangdong, China

Summary. Background. CircRNA has a covalently closed circular conformation and a stable structure. However, the exact role of circRNA in esophageal squamous cell carcinoma (ESCC) remains uncertain. The purpose of this study was to explore the role of hsa_circ_0000277 (circ_PDE3B) in ESCC.

Methods. The expression levels of circ_PDE3B, miR-136-5p and mitogen-activated protein kinase kinase kinase 2 (MAP3K2) in ESCC tissues and cells were detected by quantitative real-time polymerase chain reaction (qRT-PCR) or western blot. The proliferation ability of EC9706 and KYSE30 cells was detected by clonal formation, 5-ethynyl-2'-deoxyuridine (EdU) and 3-(4,5-dimethyl-2-thiazolyl)-2,5-diphenyl-2-H-tetrazolium bromide (MTT) assays. Flow cytometry was used to detect the apoptosis rate of cells. Transwell assay was used to detect the invasion ability of EC9706 and KYSE3 cells. The relationship between miR-136-5p and circ_PDE3B or MAP3K2 was verified by dual-luciferase reporter assay and RNA pull-down, and the effect of circ_PDE3B on tumor growth *in vivo* was explored through tumor transplantation experiment. Immunohistochemistry (IHC) assay was used to detect MAP3K2 and Ki67 expression in mice tumor tissues.

Results. The results showed that circ_PDE3B was highly expressed in ESCC tissues and cells. Down-regulated circ_PDE3B expression in ESCC cells significantly reduced cell proliferation, migration and invasion. Circ_PDE3B served as a sponge for miR-136-5p, and miR-136-5p inhibition reversed the roles of circ_PDE3B knockdown in ESCC cells. MAP3K2 was a direct target of miR-136-5p, and miR-136-5p targeted MAP3K2 to inhibit the malignant behaviors of ESCC cells. Furthermore, circ_PDE3B regulated MAP3K2 expression by sponging miR-136-5p. Importantly, circ_PDE3B knockdown inhibited tumor growth *in vivo*.

Conclusions. In conclusion, circ_PDE3B acted as oncogenic circRNA in ESCC and accelerated ESCC progression by adsorption of miR-136-5p and activation of MAP3K2, supporting circ_PDE3B as a potential therapeutic target for ESCC.

Key words: Esophageal cancer, circ_PDE3B, miR-136-5p, MAP3K2, Proliferation

Introduction

Esophageal cancer is a common type of cancer (Smyth et al., 2017). Esophageal squamous cell carcinoma is the most common histological type of esophageal carcinoma in China (Yang et al., 2019). At present, the main treatment methods are surgery and chemotherapy, and due to its high recurrence rate and high invasiveness the 5-year survival rate is only 15-25% (Huang and Yu, 2018). Therefore, it is extremely urgent to find suitable molecular markers for early diagnosis and treatment and to improve the 5-year survival rate of ESCC patients.

CircRNAs are emerging as a new star in the field of non-coding RNAs and have become a hot research direction of potential molecular biomarkers for cancer diagnosis, treatment and prognosis in recent years (Geng et al., 2018). CircRNAs are circular structures by linking free 3'- to 5'- ends and are more stable than mRNAs or linear non-coding RNAs and do not contain RNA exonucleases (Barrett and Saltzman, 2016). CircRNAs not only exist in cells, but also can be delivered to play a role outside the cell (Li et al., 2015). This property of circRNA allows it to be used as a biomarker for testing samples by entering the blood, and more importantly, circRNAs have been shown to be able to express in specific cell types or specific pathological conditions (Zhang and Xin, 2018). In addition, there is increasing evidence that circRNAs have been identified as diagnostic or prognostic biomarkers of cancer, such as

Corresponding Author: Gang Hui, Department of Thoracic Surgery, Peking University Shenzhen Hospital, No.1120 Lianhua Road, Shenzhen, Guangdong Province, China. e-mail: doctorhui1970@163.com

www.hh.um.es. DOI: 10.14670/HH-18-567

glioma (Zhu et al., 2017) and laryngeal squamous cell carcinoma (Yao et al., 2017). However, information on circRNAs as biomarkers in ESCC remains to be explored. Studies have shown that circ_PDE3B was elevated in ESCC tumor tissues and cells and promoted the progression of ESCC (Zhou et al., 2021a). Nevertheless, the precise function and mechanism of circ_PDE3B in ESCC are still largely unknown.

It is well known that circRNAs are rich in microRNA (miRNA)-binding sequence and function as sponges for miRNAs, thereby affecting target gene expression (Panda, 2018; Bach et al., 2019). Dysregulation of miRNAs is tightly related to the progression of cancer (Kwan et al., 2016). MiR-136-5p can act as a tumor-suppressing miRNA in some cancers (Liang et al., 2021a; Yang et al., 2021). MiR-136 has been reported to be downregulated in ESCC (Huang et al., 2019). Moreover, mitogen-activated protein kinase kinase kinase 2 (MAP3K2) serves as a tumor-promoting gene in multiple human malignancies (Liu et al., 2020; Li et al., 2021). However, its role in ESCC has not been explored. Intriguingly, bioinformatics analysis predicted that circ_PDE3B and MAP3K2 had complementary binding sites for miR-136-5p. Based on these findings, we assumed that circ_PDE3B might affect ESCC development by regulating circ_PDE3B and MAP3K2.

In this study, the relationship between circ_PDE3B, miR-136-5p and MAP3K2 and their influence on the progression of ESCC were studied, laying a foundation for the search for novel ESCC tumor biomarkers and therapeutic targets.

Materials and methods

Clinical tissue samples

Specimens of surgically resected esophageal squamous cell carcinoma and adjacent normal tissues from 41 patients admitted to Peking University Shenzhen Hospital were collected. All patients signed written informed consent and the study was approved by the Peking University Shenzhen Hospital ethics committee.

Cell culture and transfection

Human esophageal epithelial cells: HET-1A, and human esophageal cancer cell lines: EC9706 and KYSE30 were obtained from the Cell Bank of Chinese Academy of Sciences (Shanghai, China). All cells were cultured with Dulbecco's Modified Eagle Medium (DMEM; Invitrogen, Carlsbad, CA, USA) containing 10% fetal bovine serum (FBS; Invitrogen) and 1% double antibody (Invitrogen). The culture condition was 37°C, 5% CO_2.

Short hairpin RNA targeting circ_PDE3B (sh-circ_PDE3B) and matched control (sh-NC), miR-136-5p mimic and inhibitor (miR-136-5p and anti-miR-136-5p) and matched controls (miR-NC and anti-miR-NC), MAP3K2 overexpression plasmid (MAP3K2) and marched control (pcDNA) were provided by RiboBio (Guangzhou, China). Lipofectamine 3000 (Invitrogen) was used for transfection.

Quantitative real-time polymerase chain reaction (qRT-PCR)

TRIzol reagent (Invitrogen) was used to extract total RNA from tissues and cells, and total RNA was reversely transcribed into cDNA template according to the reverse transcription kit (TaKaRa, Kusatsu, Japan). QRT-PCR was performed according to the instructions of SYBR Premix Ex Taq II kit (TaKaRa). Relative expression was calculated by $2^{-\Delta\Delta Ct}$ method, followed by normalization to GAPDH (for circRNA or mRNA) or U6 (for miRNA). The sequence information of primers is listed in Table 1.

Table 1. Primers sequences used for PCR.

Name	Primers (5'-3')	
circ_PDE3B (hsa_circ_0000277)	Forward	CCAAGAATTTGGCATTTCAAGATGA
	Reverse	TGACACCATATTGCGAGCCT
PDE3B	Forward	TCCTGATACTGCTGATTTTCTTA
	Reverse	GTCTTTCTTCTCTGTTTCCTCTT
MAP3K2	Forward	TGGAGTGTTGCATGTACTGTGGT
	Reverse	GTTTGTTGGCTGAGTGGCGATTT
miR-136-5p	Forward	GTATGAACTCCATTTGTTTTG
	Reverse	TGGTGTCGTGGAGTCG
GAPDH	Forward	GGAGCGAGATCCCTCCAAAAT
	Reverse	GGCTGTTGTCATACTTCTCATGG
U6	Forward	GCTTCGGCAGCACATATACTAA
	Reverse	AACGCTTCACGAATTTGCGT
circ_104811 (hsa_circ_0087378)	Forward	GTCTATGCTGTGGTGGTGAT
	Reverse	TACTTCTGTTCGTGGTGTCC
circ_100933 (hsa_circ_0023984)	Forward	GTATATTACTCTACATTGTCCCAG
	Reverse	TCTAAATTAGTTTGATACTTCAGC
miR-1200	Forward	GTATGACTCCTGAGCCATTC
	Reverse	TGGTGTCGTGGAGTCG
miR-1294	Forward	GTATGATGTGAGGTTGGCAT
	Reverse	TGGTGTCGTGGAGTCG
miR-421	Forward	GTATGAATCAACAGACATTAA
	Reverse	TGGTGTCGTGGAGTCG
miR-571	Forward	GTATGATGAGTTGGCCATC
	Reverse	TGGTGTCGTGGAGTCG
miR-873-5p	Forward	GTATGAGCAGGAACTTGTG
	Reverse	TGGTGTCGTGGAGTCG
HOXB2	Forward	TGAATTTGAGAGGGAGATTGGGT
	Reverse	GGCTGGAGGCTGGGGAAGGTTTG
DEC2 (BHLHE41)	Forward	GGACTGGACTATTCCTCTTTGT
	Reverse	ATTATCTTCTGATGCTGTTGCT
HMGA2	Forward	AGGCAGACCTAGGAAATGGC
	Reverse	CCTAGTCCTCTTCGGCAGAC

Subcellular localization assay

PARIS™ Kit (Invitrogen) was applied for isolating cytoplasmic and nuclear RNAs. The expression levels of circ_PDE3B, GAPDH and U6 were determined by qRT-PCR. U6 or GAPDH functioned as a nucleus control or cytoplasm control, respectively.

RNase R and Actinomycin D assay

The RNA was divided into RNase R digestion group (RNase R+) and non-digestion group (RNase R-). In RNase R+ group, 1μg RNA was added with the ratio of 1U RNase RNase R (Seebio, Shanghai, China), and mixed at 37°C for 15 min. Then the digested products were extracted with benzene chloroform precipitation method and reversely transcribed into cDNA. QRT-PCR was used for the results.

The cells were co-cultured with Actinomycin D (Sigma, St. Louis, MO, USA), and RNA at different time nodes were obtained and related expressions were measured by qRT-PCR.

Colony formation experiment

Transfected EC9706 and KYSE30 cells were inoculated into 6-well plates at a rate of 5×10^2/ well, evenly dispersed and then placed in cell culture boxes. Cells were observed once every day, and culture was terminated when cell colonies were seen in the plates at about 14 days. The cell colonies were fixed with formaldehyde (Sigma) for 15 min and stained with Giemsa (Beyotime, Jiangsu, China) for 30 min. Statistical observation was performed under a microscope (Leica, Wetzlar, Germany).

5-Ethynyl-2'-deoxyuridine (EdU) test

BeyoClick™ EdU Cell Proliferation Kit (Beyotime) was used for EdU assay. After transfection, the cells in each group were inoculated into a 24-well cell culture plate, and incubated in medium containing 50 μmol EdU for 48h. The cells were fixed with iced methanol at room temperature for 15 min. These cells were then permeated using 0.5% Triton-X-100, followed by incubation with reaction mixture for 30 min in a dark place. Thereafter, DAPI was used to stain the nucleic acids. Lastly, EdU-positive cells were observed under a fluorescence microscope (Leica).

3-(4,5-dimethylthiazol-2-yl)-2,5-diphenyltetrazolium bromide (MTT) assay

The transfected EC9706 and KYSE30 cells were inoculated into 96-well plates according to the ratio of 5×10^3/ well. After 48h, 20 μL MTT (Beyotime) solution was added to each well. After 4h, 150 μL dimethyl sulfoxide was added to each well, and the cells were shaken into crystallized solution for 10 min. The absorbance (OD) value at wavelength 570 nm was detected by a microplate reader (Bio-Rad, Hercules, CA, USA).

Flow cytometry

Annexin V-fluorescein isothiocyanate (FITC)/ propidium iodide (PI) apoptosis detection kit (Sigma) was used to measure cell apoptosis. The transfected cells were cultured in 6-well cell culture plates for 48 h and collected. The cells were centrifuged at 1000 r/min at 4°C for 5 min. The supernatant was discarded and washed with PBS buffer for 3 times. Next, cells were suspended in binding buffer and incubated with Annexin V-FITC and PI for 20 min in the dark. The apoptosis rate of each group was detected by flow cytometry (BD Biosciences, Franklin Lakes, NJ, USA).

Transwell assay

Transfected cells (2×10^5 cells) were respectively added to the upper chamber of Transwell chamber. The upper chamber was coated with 10% Matrigel (BD Biosciences) for 0.5h at 37°C to detect invasion ability, and the non-coated cells were tested for migration ability. 600 μL RPMI 1640 medium containing 10% FBS was added into the lower chamber. After being routinely cultured for 48 h, the cells on the upper side of the membrane were wiped with cotton swabs, cleaned with PBS and stained with crystal violet (Beyotime). Routine preparation was performed and observed under inverted phase contrast microscope (×200) and photographed.

Western blot

RIPA lysis buffer (Beyotime) was utilized for extracting total protein, and the proteins were denatured via heating for 3-5 min at 100°C. After determination of protein concentration with BCA protein assay kit (Abcam, Cambridge, MA, USA), the proteins (40 μg/lane) were separated by polyacrylamide gel electrophoresis (SDA-PAGE) for 2h and wetted for 2h. The proteins were transferred to polyvinylidene fluoride (PVDF) membrane. The specific primary antibody was incubated with PVDF membrane at 4°C overnight. The PVDF membrane was cleaned with TBST 3 times, 5 min each time. The second antibody was added and the PVDF membrane was incubated at room temperature for 2h, and then the PVDF membrane was cleaned with TBST 3 times, with each cleaning for 5 min. The protein signals were visualized using enhanced chemi-luminescence (ECL) chromogenic substrate (Abcam) in the dark. The antibodies including Snail (1:2000, ab216347), GAPGH (1:2000, ab37168), MAP3K2 (1:1000, ab33918), and HRP-conjugated IgG anti-rabbit (1:4000, ab205718) were purchased from Abcam, and Twist1 (1:1000, 25465-1-AP) and E-cadherin (1:2000, 20874-1-AP) were bought from Proteintech (Rosemont,

IL, USA).

Dual-luciferase reporter assay

Circ_PDE3B and 3'UTR of MAP3K2 fragments containing miR-136-5p binding site region and the corresponding mutated region were amplified and individually cloned into the pmirGlO luciferase reporter vector (Promega, Madison, WI, USA) to generate circ_PDE3B-WT, circ_PDE3B-MUT, MAP3K2-WT, and MAP3K2-MUT vectors. EC9706 and KYSE30 cells were inoculated with 4.5×10^4 cells/well in 24-well plates and cultured until 70% fusion. EC9706 and KYSE30 cells were then co-transfected with miR-136-5p or miR-NC and generated luciferase reporter vector. After transfection 48h, luciferase activity was determined using dual-Luciferase Reporter Assay System (Promega).

RNA pull-down

EC9706 and KYSE30 cells incubated with biotinylated wild-type (WT) or mutant (MUT) circ_PDE3B/MAP3K2 (Bio-circ_PDE3B-WT, Bio-circ_PDE3B-MUT, Bio- MAP3K2-WT, and Bio-MAP3K2-MUT) or negative control (Bio-NC) were lysed with RIP buffer. The lysates were combined with M-280 streptavidin magnetic beads (Invitrogen). The expression level of miR-136-5p was detected by qRT-PCR.

Xenograft tumor

All animal testing protocols were completed under the supervision and approval of the Peking University Shenzhen Hospital Animal Ethics Committee. Ten BALB/c nude mice provided by Vital River Laboratory Animal Technology Co., Ltd (Beijing, China) were divided into two groups. EC9706 cells stably transfected with sh-NC or sh-circ_PDE3B were injected respectively. The tumor volume was measured every five days starting from day 10 and calculated using the formula: $1/2\times width^2\times length$. The tumor tissues were removed 30 days later and the weight was measured. QRT-PCR, western blot and immunohistochemistry (IHC) assays were used to detect the expression of related factors.

IHC analysis

Tumor tissues from nude mice were fixed in formaldehyde (10%), embedded in paraffin, and cut into 4-μm-thick sections. Afterwards, these sections were incubated with the primary antibody: MAP3K2 (1:200, ab33918, Abcam) or Ki67 (ab15580, 1:200, Abcam), followed by incubation with secondary antibody (ab205718, 1:2000, Abcam). After staining with diaminoaniline (DAB; Beyotime) and counterstaining with haematoxylin (Beyotime), a microscope (Leica) was used to observe the immunofluorescence images.

Statistical analysis

Statistical analysis was performed using SPSS 23.0 (SPSS Inc., Chicago, IL, USA). Results are reported as mean ± standard deviation. Comparisons were made using student's t test or one-way ANOVA. Pearson's correlation coefficient was used to analyze the correlations among circ_PDE3B, miR-136-5p and MAP3K2 in ECSS tissues. Statistical significance was considered when $P<0.05$.

Results

Circ_PDE3B expression in ESCC tissues and cell lines

As shown in Fig. 1A,B, we selected 3 circRNAs (circ_PDE3B, circ_104811 and circ_100933) with a significant difference from GSE131969 data analysis. The expression of circ_PDE3B in GSE131969 data is presented in Fig. 1C. QRT-PCR was used to detect the expression of circ_PDE3B, circ_104811 and circ_100933 in EC9706 and KYSE30 cells compared with HET-1A cells, and it was found that circ_PDE3B showed the largest difference (Fig. 1D). As revealed from the outcomes, circ_PDE3B expression in ESCC tissues was conspicuously higher than that in normal control (Fig. 1E). Fig. 1F,G show that circ_PDE3B was mainly distributed in the cytoplasm of EC9706 and KYSE30 cells. Digestion with RNase R exonucleases confirmed that circ_PDE3B is more stable than PDE3B mRNA, as shown in Fig. 1H,I. The results of actinomycin D assays revealed that the half-life of the circ_PDE3B transcript was longer than the half-life of the PDE3B mRNA (Fig. J,K). These results indicated that circ_PDE3B might play an important role in ESCC progression.

Circ_PDE3B knockdown had a tumor suppressive effect on ESCC cells in vitro

QRT-PCR was used to measure the transfection effect of sh-circ_PDE3B in EC9706 and KYSE30 cells, and the results displayed that the content of circ_PDE3B was prominently reduced, while the level of PDE3B mRNA was not affected (Fig. 2A,B). The clone formation experiment, EdU experiment and the MTT experiment showed that after suppression of circ_PDE3B, the proliferation ability of EC9706 and KYSE30 cells was remarkably diminished (Fig. 2C-F). Flow cytometry revealed that silencing circ_PDE3B apparently facilitated the cell apoptotic rate (Fig. 2G). The result of the transwell assays showed that the downregulation of circ_PDE3B blocked cell migration and invasion (Fig. 2H,I). Circ_PDE3B silencing inhibited Snail and Twist1 protein levels and promoted E-cadherin protein expression (Fig. 2J,K). Collectively, these data indicated that downregulation of circ_PDE3B

suppressed the progression of ESCC cells.

Circ_PDE3B performed its function by sponging miR-136-5p

The miRNAs that may interact with circ_PDE3B in both Circinteractome (https://circinteractome.nia.nih.gov/) and Circbank (http://www.circbank.cn/) databases were screened by Venn diagram. As shown in Fig. 3A, six miRNAs may interact with circ_PDE3B, including miR-1200, miR-1294, miR-136-5p, miR-421, miR-571 and miR-873-5p. QRT-PCR data showed that the abundance of miR-1294, miR-136-5p and miR-873-5p in EC9706 and KYSE30 cells was evidently diminished compared with that in HET-1A cells (Fig. 3B). Fig. 3C,D implied that circ_PDE3B knockdown led to a significant elevation in the expression levels of miR-136-5p and miR-873-5p in both EC9706 and KYSE30 cells, especially miR-136-5p, so miR-136-5p was selected for further analysis. The binding site of miR-136-5p to circ_PDE3B was then predicted by Circinteractome (Fig. 3E). As shown in Fig. 3F,G, miR-136-5p was only able to reduce the luciferase activity of circ_PDE3B-WT, but not circ_PDE3B-MUT. RNA pull-down results suggested that Bio-circ_PDE3B-WT prominently enriched miR-136-5p (Fig. 3H). The abundance of miR-136-5p was significantly reduced in ESCC tissues (Fig. 3I). MiR-136-5p and circ_PDE3B expression levels in ESCC tissues were negatively correlated (Fig. 3J). In summary, circ_PDE3B was able to bind with miR-136-5p in ESCC cells.

MiR-136-5p inhibitor reversed the effects of circ_PDE3B knockdown on proliferation, migration, invasion and apoptosis of ESCC cells

Circ_PDE3B knockdown markedly enhanced the expression of miR-136-5p, while miR-136-5p inhibitor

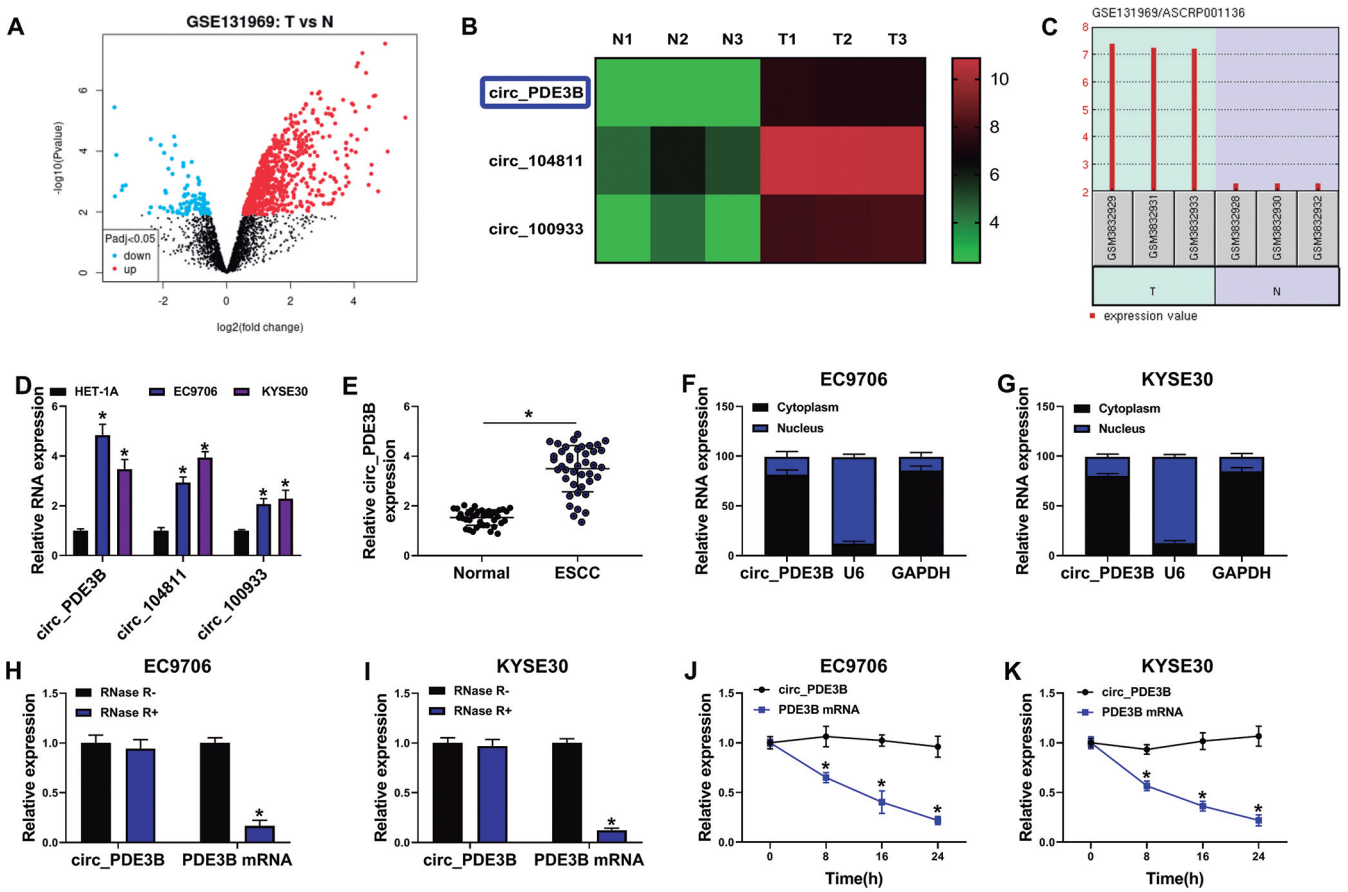

Fig. 1. Expression of circ_PDE3B in ESCC tissues and cells. **A.** Volcano plots show the expression of circRNAs in ESCC cancerous tissues with adjacent normal tissues (GSE131969). **B.** Clustered heat map of the differentially expressed circRNAs in three human ESCC cancerous tissues and adjacent normal tissues (GSE131969). **C.** The differential expression of circ_PDE3B was analyzed by GSE131969 database. **D.** QRT-PCR was used to detect circ_PDE3B, circ_104811 and circ_100933 levels in ESCC cells. (E) QRT-PCR was applied to assess circ_PDE3B expression in ESCC tissues. **F and G.** Expression levels of circ_PDE3B, U6, and GAPDH in the cell cytoplasmic and nucleus were determined by qRT-PCR in EC9706 and KYSE30 cells. **H and I.** QRT-PCR analysis revealed the expression of circ_PDE3B, PDE3B in EC9706 and KYSE30 cells treated with or without RNase R. **J and K.** Expression of PDE3B mRNA level and circ_PDE3B in EC9706 and KYSE30 cells treated with actinomycin D. *P<0.05.

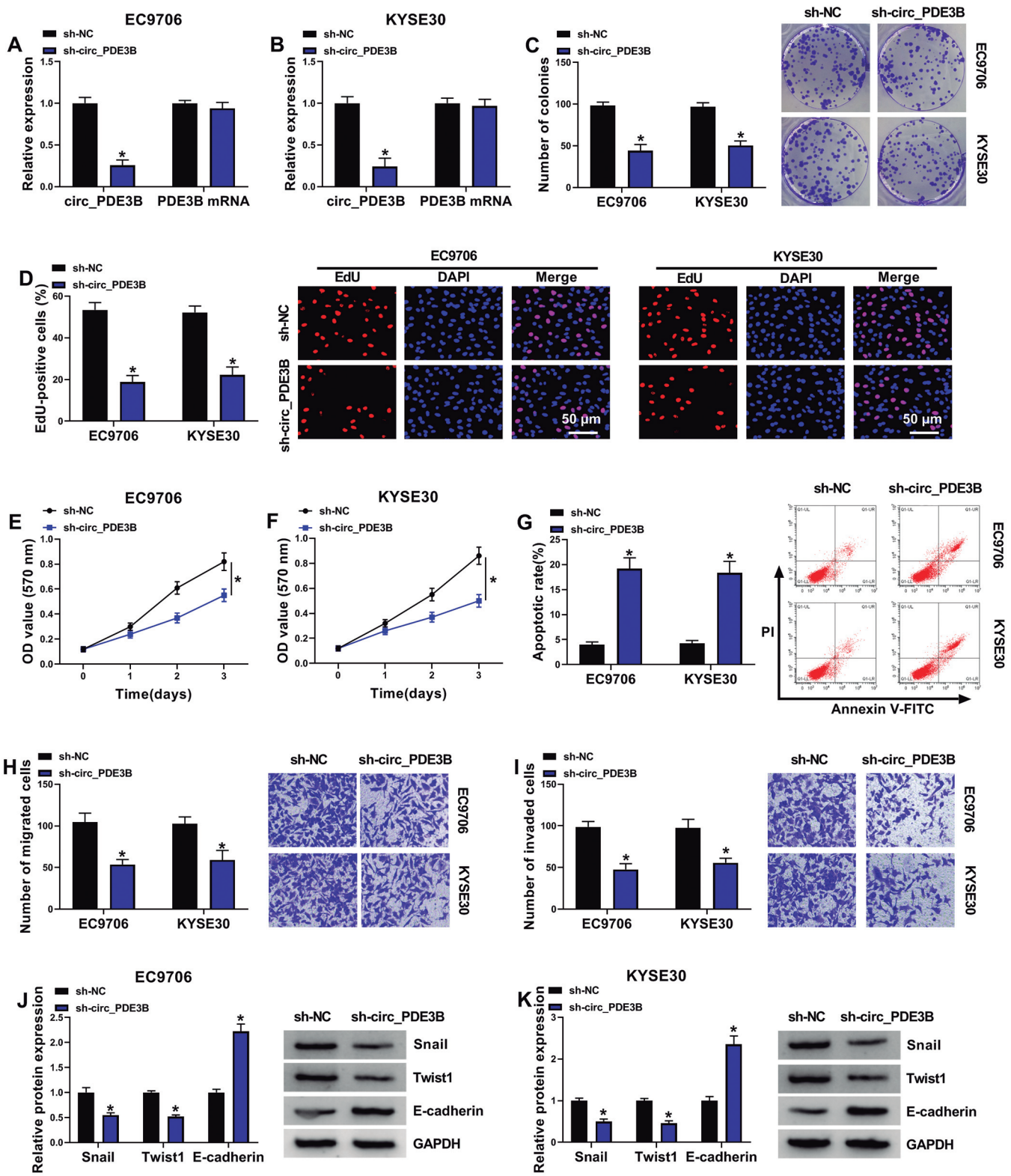

Fig. 2. Influence of circ_PDE3B inhibition on proliferation, migration, invasion, and apoptosis of ESCC cells. **A and B.** QRT-PCR revealed the expression of circ_PDE3B in EC9706 and KYSE30 cells transfected with sh-NC or sh-circ_PDE3B. **C-F.** The colony formation, cell proliferation, cell viability of EC9706 and KYSE30 cells were determined by colony formation assay, EdU assay, or MTT assay. **G.** The apoptotic rate of EC9706 and KYSE30 cells was examined by flow cytometry assay. **H and I.** The migration and invasion of EC9706 and KYSE30 cells was analyzed by transwell assay. **J and K.** Western blotting presented the levels of Snail, Twist1 and E-cadherin protein in EC9706 and KYSE30 cells. *P<0.05.

attenuated this change (Fig. 4A). Inhibition of circ_PDE3B impeded EC9706 and KYSE30 cell proliferation, but this inhibitory effect was reversed by anti-miR-136-5p (Fig. 4B-E). Silencing of circ_PDE3B promoted the apoptotic rate of EC9706 and KYSE30 cells, while sh-circ_PDE3B and anti-miR-136-5p co-transfection counteracted this effect (Fig. 4F). The inhibition of circ_PDE3B silencing on the migration and invasion of EC9706 and KYSE30 cells was restored by miR-136-5p inhibition (Fig. 4G,H). The inhibition of circ_PDE3B silencing on Snail and Twist1 proteins and the promotion on E-cadherin protein were weakened by anti-miR-136-5p (Fig. 4I,J). Altogether, these data indicated that circ_PDE3B regulated ESCC cell proliferation, apoptosis, migration, and invasion by sponging miR-136-5p.

Circ_PDE3B regulated MAP3K2 by targeting miR-136-5p

MiR-136-5p expression was diminished in EC9706 and KYSE30 cells transfected with miR-136-5p inhibitor and increased in EC9706 and KYSE30 cells transfected with miR-316-5p mimic (Fig. 5A). The target genes of miR-136-5p were predicted by Starbase3.0 (http://starbase.sysu.edu.cn/). Common highly expressed target genes were searched in the literature, then HOXB2, DEC2, MAP3K2 and HMGA2 were screened. QRT-PCR displayed that MAP3K2 mRNA expression was significantly reduced in EC9706 and KYSE30 cells transfected with miR-136-5p, and significantly increased in the cells transfected with anti-miR-136-5p (Fig. 5B,C). As shown in Fig. 5D, miR-136-5p over-expression dramatically reduced MAP3K2 protein level

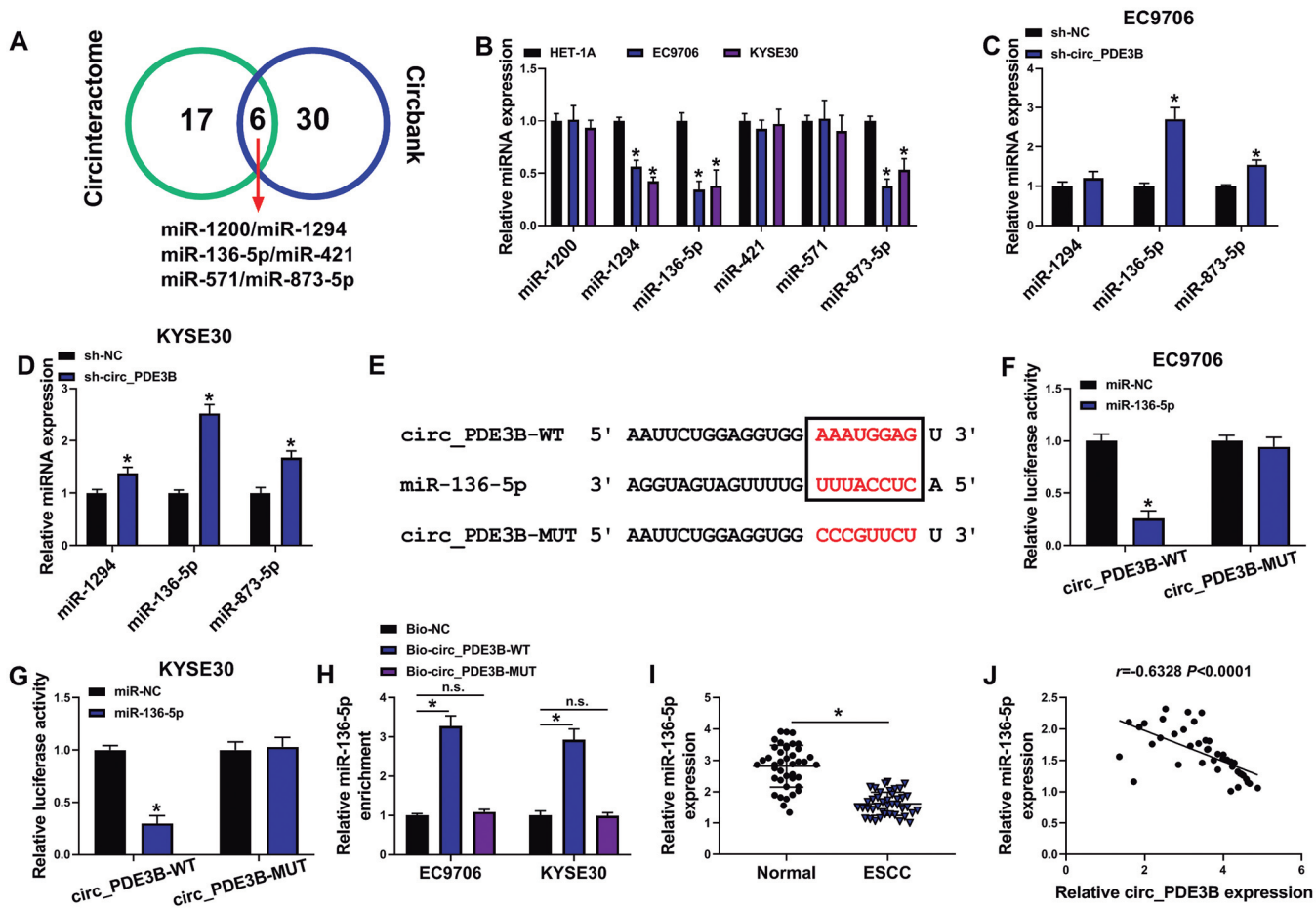

Fig. 3. Circ_PDE3B served as a sponge for miR-136-5p in ESCC cells. **A.** The intersection of miRNAs targeting circ_PDE3B predicted by Circinteractome and Circbank is shown in the Venn diagram. **B.** The expression of miR-1200, miR-1294, miR-136-5p, miR-421, miR-571, and miR-873-5p was detected by qRT-PCR. **C and D.** The levels of miR-1294, miR-136-5p, and miR-873-5p in EC9706 and KYSE30 cells were measured by qRT-PCR after being transfected with sh-circ_PDE3B or sh-NC. **E.** Circinteractome predicted a complementary site between circ_PDE3B and miR-136-3p. **F and G.** Dual-luciferase reporter assay was carried out to analyze the luciferase activity of the luciferase reporter containing circ_PDE3B-WT or circ_PDE3B-MUT. **H.** We used RNA pull-down to further examine the relationship between miR-136-5p and circ_PDE3B in EC9706 and KYSE30 cells. **I.** QRT-PCR analyzed the expression of miR-136-5p in ESCC tissues. **J.** Linear correlation between miR-136-5p and circ_PDE3B expression was analyzed by Pearson's correlation coefficient. *P<0.05.

in EC9706 and KYSE30 cells, but miR-136-5p inhibition had an opposite influence. The binding site of miR-136-5p to MAP3K2 was predicted by Starbase3.0 (Fig. 5E). We observed that miR-136-5p restrained the luciferase activity of EC9706 and KYSE30 cells in the MAP3K2-WT group, but not in the MAP3K2-MUT group (Fig. 5F,G). Moreover, miR-136-5p was markedly enriched in the Bio-MAP3K2-WT group (Fig. 5H). The expression of MAP3K2 both on mRNA and protein levels was enhanced in ESCC tissues (Fig. 5I,J). Pearson's correlation coefficient implicated that MAP3K2 expression was negatively correlated with miR-136-5p level, and positively correlated with circ_PDE3B level (Fig. 5K,L). MAP3K2 expression level was increased in ESCC cells as well (Fig. 5M,N). Circ_PDE3B knockdown decreased the mRNA and protein expression of MAP3K2 in EC9706 and KYSE30 cells, and the addition of miR-136-5p inhibitor largely recovered the mRNA and protein expression of MAP3K2 (Fig. 5O,P). Together, these data suggested that miR-136-5p directly targeted MAP3K2 in ESCC cells.

MiR-136-5p regulated proliferation, migration and invasion of ESCC cells through targeting MAP3K2

After MAP3K2 introduction, the decrease of MAP3K2 mRNA and protein in EC9706 and KYSE30 cells induced by miR-136-5p was partially rescued (Fig. 6A,B). Moreover, enhancement of miR-136-5p impeded proliferation and facilitated apoptosis of EC9706 and KYSE30 cells, but these effects were abolished by MAP3K2 overexpression (Fig. 6C-G). Also, elevated MAP3K2 expression abrogated the inhibitory effect of miR-136-5p mimic on migration and invasion of EC9706 and KYSE30 cells (Fig. 6H,I). Additionally, overexpression of MAP3K2 recovered the diminished Snail and Twist1 proteins and the elevated E-cadherin protein in miR-136-5p-increased EC9706 and KYSE30 cells (Fig. 6J,K). All findings indicated that miR-136-5p exerted the anti-cancer role by targeting MAP3K2 in ESCC cells.

Circ_PDE3B downregulation blocked tumor growth in vivo

Compared with the sh-NC group, tumor volume and weight were reduced in sh-circ_PDE3B group (Fig. 7A,B). The abundance of circ_PDE3B in xenograft tumor tissues was suppressed and the content of miR-136-5p was elevated by sh-circ_PDE3B (Fig. 7C,D). Both MAP3K2 mRNA and protein levels were restrained by sh-circ_PDE3B in xenograft tumor tissues (Fig. 7E,F). Moreover, circ_PDE3B silencing reduced MAP3K2 and Ki-67 expression (Fig. 7G). These results uncovered that circ_PDE3B knockdown inhibited tumor

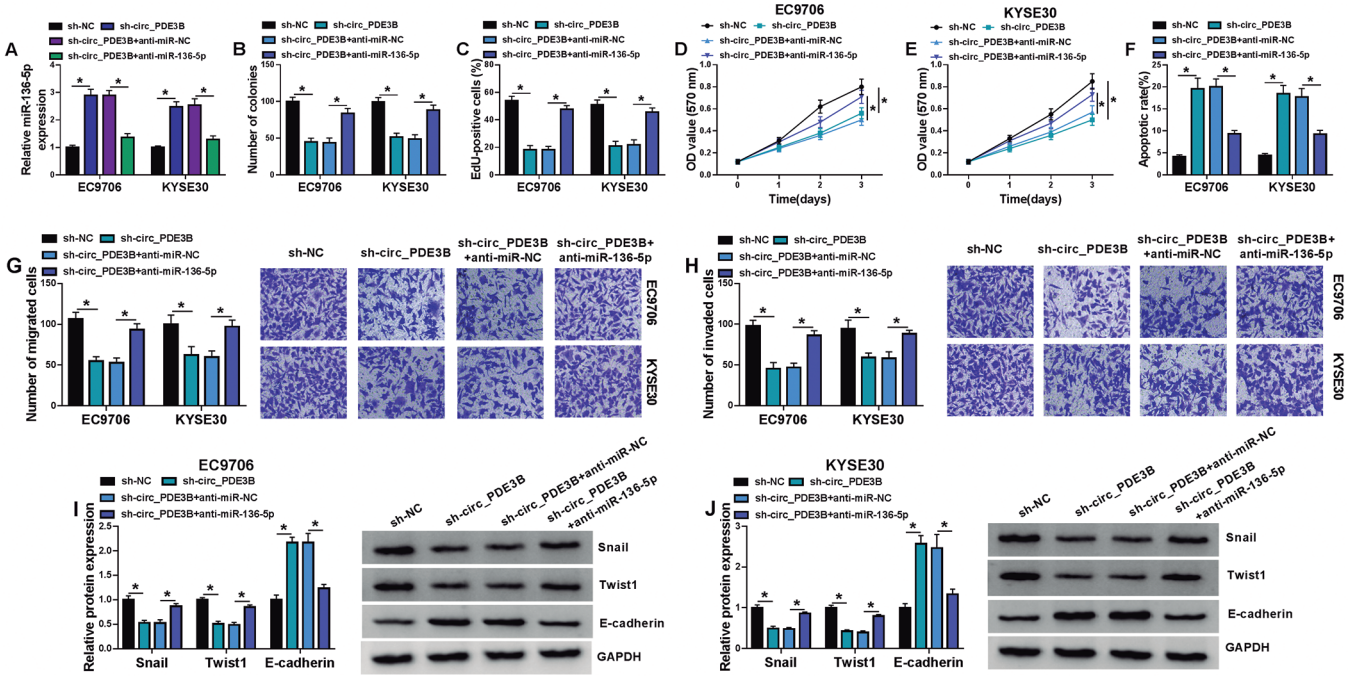

Fig. 4. Circ_PDE3B affected malignant behaviors of ESCC cells by sponging miR-136-5p. EC9706 and KYSE30 cells were transfected with sh-NC, sh-circ_PDE3B, sh-circ_PDE3B+anti-miR-NC, or sh-circ_PDE3B+anti-miR-136-5p. **A.** Expression of miR-136-5p in EC9706 and KYSE30 cells was evaluated using qRT-PCR. **B-F.** Colony formation, cell proliferation, cell viability, and apoptosis were determined by using colony formation assay, EdU assay, MTT assay, and flow cytometry assay, respectively. **G and H.** Cell migration and invasion were demonstrated by using transwell assay. **I and J.** The levels of Snail, Twist1 and E-cadherin protein were analyzed using western blot. *P<0.05.

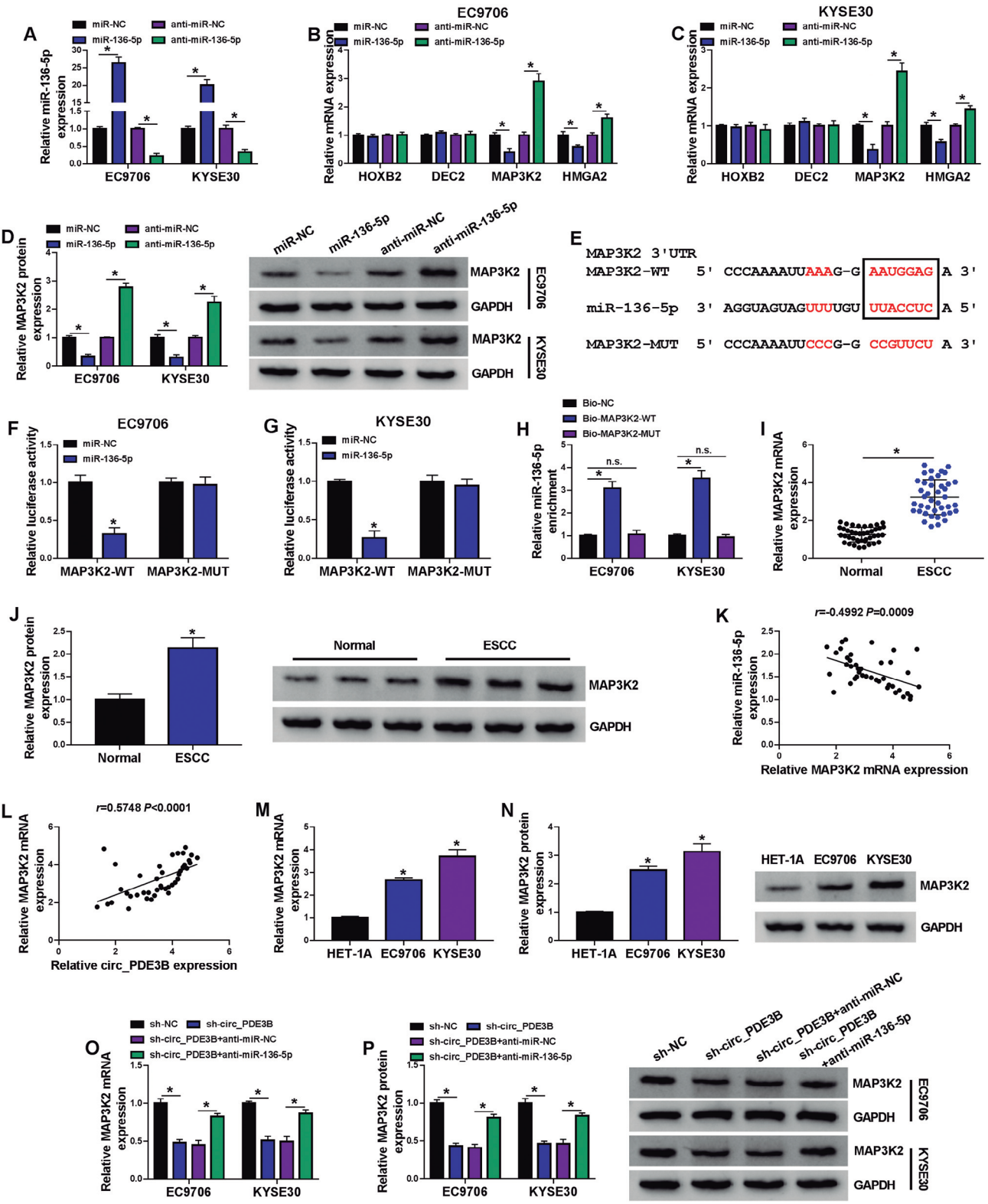

Fig. 5. Circ_PDE3B regulated MAP3K2 expression via sponging miR-136-5p in ESCC cells. **A.** The expression of miR-136-5p in EC9706 and KYSE30 cells transfected with miR-NC, miR-136-5p, anti-miR-NC or anti-miR-136-5p was examined by qRT-PCR. **B and C.** QRT-PCR was used for testing the levels of HOXB2, DEC2, MAP3K2 and HMGA2. **D.** MAP3K2 protein expression in transfected ESCC cells was analyzed by western blot assay. **E.** The interaction between MAP3K2 and miR-136-5p was predicted by Starbase3.0 software. **F and G.** The target interaction between miR-136-5p and MAP3K2 was tested via dual-luciferase reporter assay. (H) RNA pull-down assay was utilized to verify the interaction between miR-136-5p and MAP3K2. **I and J.** MAP3K2 mRNA and protein expression in ESCC tissues and adjacent normal tissues was detected by qRT-PCR and western blot assay, respectively. **K and L.** Correlation between MAP3K2 and miR-136-5p or circ_PDE3B mRNA expression was analyzed using Pearson's correlation coefficient. **M and N.** QRT-PCR and western blot assay were implemented to examine the mRNA and protein expression levels of MAP3K2, respectively, in EC9706, KYSE30 and HET-1A cells. **O and P.** QRT-PCR and western blot assays were used to assess the mRNA and protein abundance of MAP3K2 in ESCC cells. *P<0.05.

growth by upregulating miR-136-5p and downregulating MAP3K2.

Discussion

ESCC is one of the familiar gastrointestinal malignancies in China, accounting for more than 90% of esophageal cancer, with a high incidence, and at present radical resection is the most effective treatment for ESCC. With the improvement of technical level, the prognosis of patients has improved, but the patient 5-year survival rate is still not satisfactory, and the prognosis has always been a concern (Zhang et al., 2018b, 2019; Samiei et al., 2019).

CircRNAs are a broad category of single-stranded RNAs, belonging to non-coding RNAs, with a wide range of expression patterns (Jeck and Sharples, 2014; Enuka et al., 2016; Liu et al., 2016). Many circRNAs are involved in the evolution of cancer, including ESCC (Zhang et al., 2018a, 2020). For example, circ_NRIP1 played a promoter role in the malignant development of ESCC through the miR-595/SEMA4D axis and the PI3K/AKT pathway (Zhou et al., 2021b). Circ-OGDH had a promoter role in ESCC glutamine metabolism and progress (Liang et al., 2021b). Liu et al. proved that silencing of hsa_circ_0014879 enhanced the ESCC radiosensitivity through regulating the miR-519-3p/CDC25A pathway (Liu et al., 2021). These reports indicated that circRNAs played an important role in the development of ESCC. However, there are few studies on the role of circ_PDE3B in cancer, and its mechanism of action is still unclear. Here, we found that

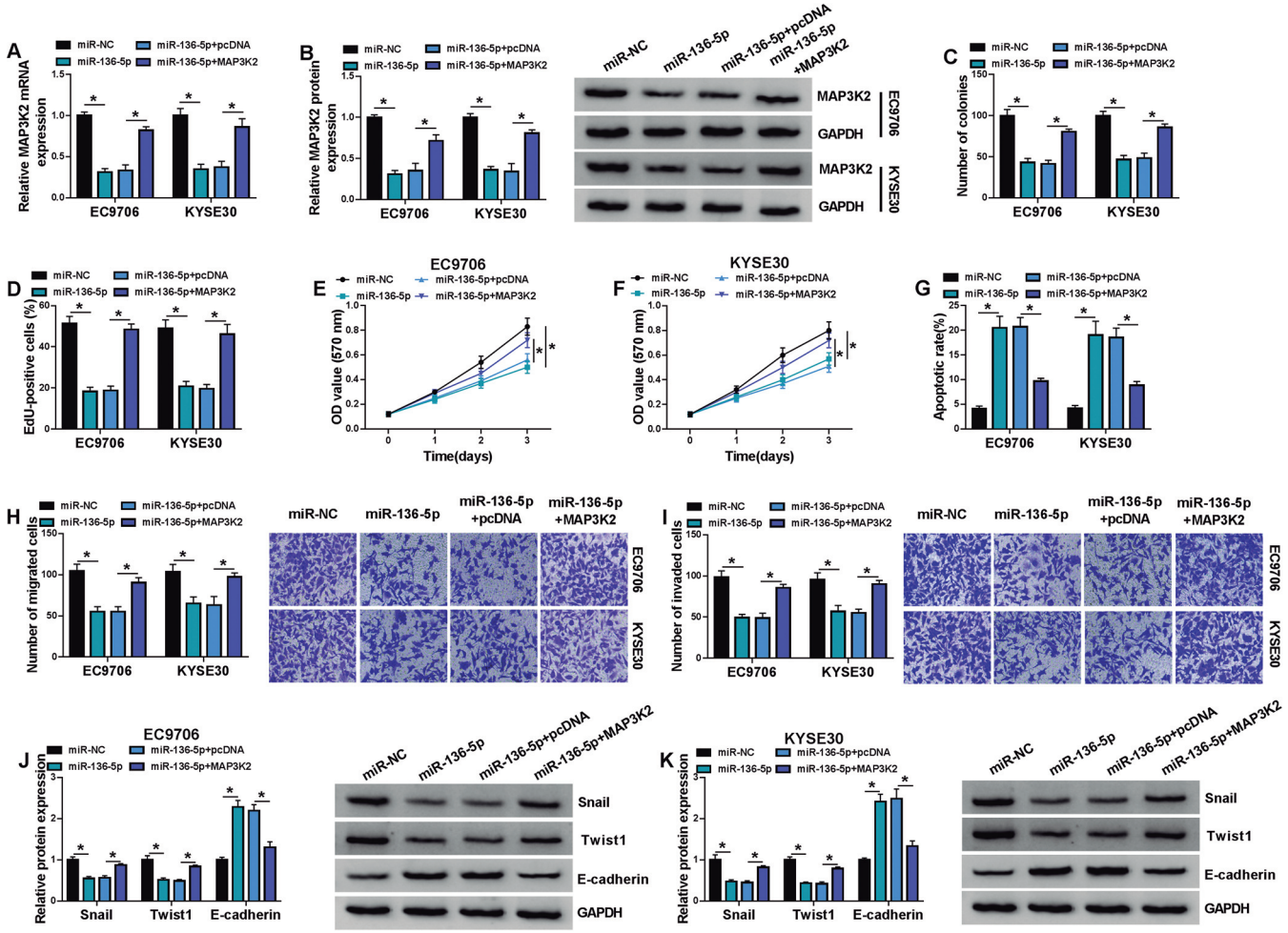

Fig. 6. MiR-136-3p-mediated influences in ESCC cells were partly reversed by the overexpression of MAP3K2. EC9706 and KYSE30 cells were transfected with miR-NC, miR-136-5p, miR-136-5p+pcDNA or miR-136-5p+MAP3K2. **A and B.** QRT-PCR and western blot assays were used to examine the mRNA and protein expression levels of MAP3K2 in ESCC cells, respectively. **C.** Colony formation assay was performed to measure the number of colonies. **D.** cell proliferation was detected by EdU assay. **E and F.** MTT assay was used to analyze the proliferative ability of EC9706 and KYSE30 cells. **G.** Flow cytometry was conducted to assess the apoptosis of EC9706 and KYSE30 cells. **H and I.** Transwell assays were conducted to assess the migration and invasion of ESCC cells. **J and K.** Protein expression levels of Snail, Twist1 and E-cadherin were detected by western blot assay. *P<0.05.

circ_PDE3B was upregulated in CSCC. Next, we knocked down circ_PDE3B expression and evaluated the effects on ESCC cell behaviors. The data showed that circ_PDE3B silencing limited ESCC cell growth, migration and invasion, and induced cell apoptosis, implying that circ_PDE3B might a play tumor-promoting role in ESCC.

Mature miRNAs are single-stranded RNA molecules with 20-23 nucleotides (nt) in length, which are important regulators of gene expression and usually reduce the stability of mRNA (Ardekani and Naeini, 2010). Previous studies have shown that miRNAs can participate in tumor formation, metastasis and metabolism by regulating the expression of downstream genes (Wu et al., 2020). MiR-136-5p played an obvious inhibitory role in a variety of malignant tumors, and its downregulated expression could lead to the occurrence and development of malignant tumors, and shorten the survival time, recurrence and distant metastasis of patients with malignant tumors (Paszek et al., 2017; Xie et al., 2018). However, the effect of circ_PDE3B on ESCC progression through miR-136-5p has not been reported. Bioinformatics analysis and dual-luciferase reporter assay showed that MAP3K2 was the target gene of miR-136-5p. Moreover, we found that miR-136-5p was downregulated in ESCC. Additionally, miR-136-5p inhibition abated the repressive influence of circ_PDE3B depletion on ESCC cell progression, indicating that circ_PDE3B regulated ESCC cell behaviors via sponging miR-136-5p.

MAP3K2 is a member of MAPK signaling pathway and can activate a series of MAP kinase signaling pathways, including c-JNK and ERK5 (Chayama et al., 2001; Su et al., 2001). Studies have shown that the content of MAP3K2 in tumor and normal cells was significantly different and promoted the progression of many tumors (Chen et al., 2019; Lv et al., 2019; Li et al., 2021). However, the role of MAP3K2 in ESCC remains unclear. In this research, an upregulation of MAP3K2 expression was found in ESCC. Moreover, MAP3K2 upregulation abated the anti-cancer role of miR-136-5p overexpression in ESCC cells, suggesting that MAP3K2 might act as an oncogene in ESCC. *In vivo* experiments further confirmed that circ_PDE3B downregulation repressed tumor growth through regulating miR-136-5p and MAP3K2 expression.

In conclusion, we detected the upregulation of circ_PDE3B in ESCC cells and tissues, and downregulation of circ_PDE3B inhibited the evolution of ESCC cells. Circ_PDE3B promoted MAP3K2

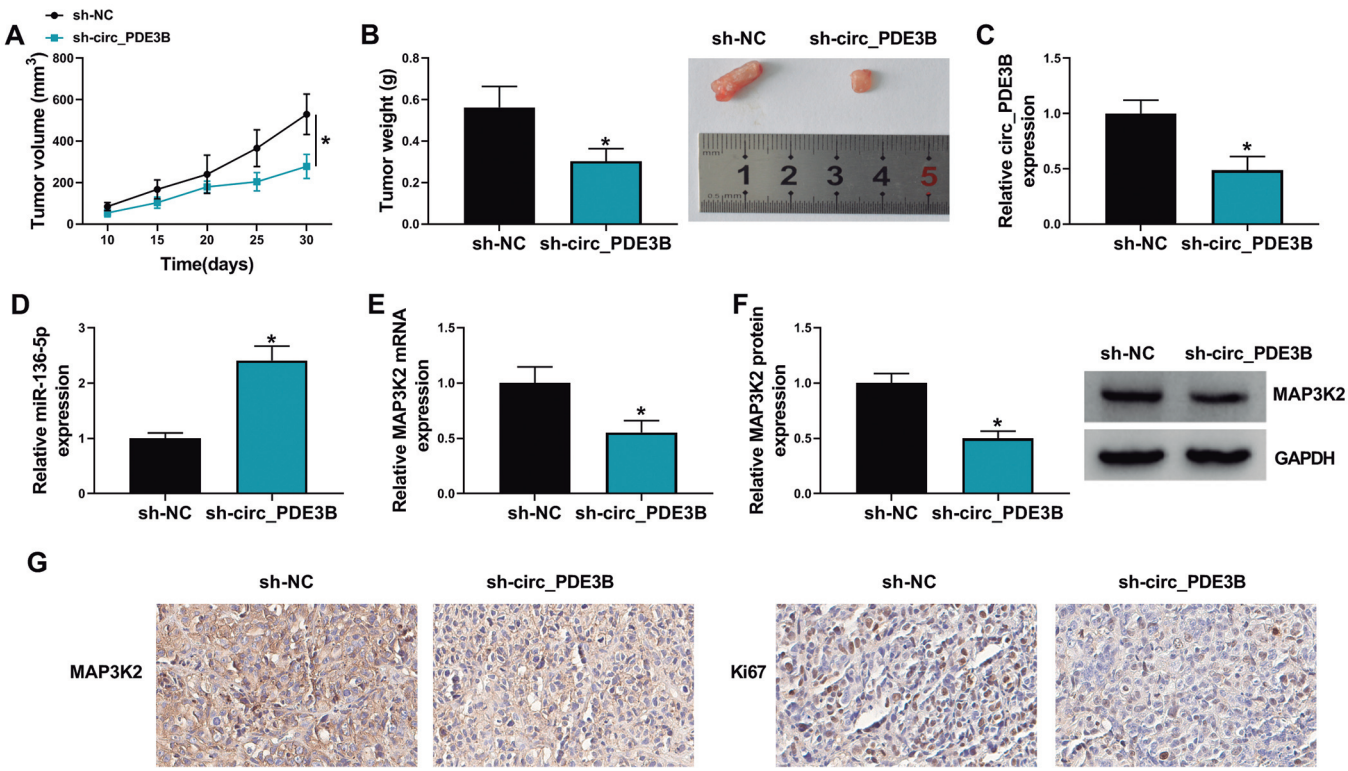

Fig. 7. Circ_PDE3B knockdown mitigated tumor growth *in vivo*. **A.** After 10 days of implantation, tumor volume measurement began and was performed every 5 days. **B.** Tumor average weight was calculated and representative pictures were photographed. **C-F.** Circ_PDE3B, miR-136-5p and MAP3K2 levels were evaluated by qRT-PCR and western blot in the xenograft tissues. **G.** IHC assay was used to detect MAP3K2 and Ki-67 expression in subcutaneously formed tumors from the sh-NC or sh-circ_PDE3B groups. *P<0.05.

expression by targeting miR-136-5p, thereby promoting ESCC tumorigenesis, suggesting that circ_PDE3B may act as a promising therapeutic target for ESCC.

Acknowledgements. None.

Disclosure of interest. The authors declare that they have no conflicts of interest.

Funding. None.

References

Ardekani A.M. and Naeini M.M. (2010). The role of microRNAs in human diseases. Avicenna J. Med. Biotechnol. 2, 161.

Bach D.H., Lee S.K. and Sood A.K. (2019). Circular RNAs in cancer. Mol. Ther. Nucleic. Acids. 16, 118-129.

Barrett S.P. and Salzman J. (2016). Circular RNAs: analysis, expression and potential functions. Development 143, 1838-1847.

Chayama K., Papst P.J., Garrington T.P., Pratt J.C., Ishizuka T., Webb S., Ganiatsas S., Zon L.I., Sun W., Johnson G.L. and Gelfand E.W. (2001). Role of MEKK2-MEK5 in the regulation of TNF-alpha gene expression and MEKK2-MKK7 in the activation of c-Jun N-terminal kinase in mast cells. Proc. Natl. Acad. Sci. USA 98, 4599-4604.

Chen X., Gao J., Yu Y., Zhao Z. and Pan Y. (2019). LncRNA FOXD3-AS1 promotes proliferation, invasion and migration of cutaneous malignant melanoma via regulating miR-325/MAP3K2. Biomed. Pharmacother. 120, 109438.

Enuka Y., Lauriola M., Feldman M.E., Sas-Chen A., Ulitsky I. and Yarden Y. (2016). Circular RNAs are long-lived and display only minimal early alterations in response to a growth factor. Nucleic Acids Res. 44, 1370-1383.

Geng Y., Jiang J. and Wu C. (2018). Function and clinical significance of circRNAs in solid tumors. J. Hematol. Oncol. 11, 98.

Huang F.L. and Yu S.J. (2018). Esophageal cancer: Risk factors, genetic association, and treatment. Asian J. Surg. 41, 210-215.

Huang H.Z., Yin Y.F., Wan W.J., Xia D., Wang R. and Shen X.M. (2019). Up-regulation of microRNA-136 induces apoptosis and radiosensitivity of esophageal squamous cell carcinoma cells by inhibiting the expression of MUC1. Exp. Mol. Pathol. 110, 104278.

Jeck W.R. and Sharpless N.E. (2014). Detecting and characterizing circular RNAs. Nat. Biotechnol. 32, 453-461.

Kwan J.Y., Psarianos P., Bruce J.P., Yip K.W. and Liu F.F. (2016). The complexity of microRNAs in human cancer. J. Radiat Res. 57 Suppl. 1, i106-i111.

Li Y., Zheng Q., Bao C., Li S., Guo W., Zhao J., Chen D., Gu J., He X. and Huang S. (2015). Circular RNA is enriched and stable in exosomes: a promising biomarker for cancer diagnosis. Cell Res. 25, 981-984.

Li X., Azhati B., Wang W., Rexiati M., Xing C. and Wang Y. (2021). Circular RNA UBAP2 promotes the proliferation of prostate cancer cells via the miR-1244/MAP3K2 axis. Oncol. Lett. 21, 486.

Liang M., Yao W., Shi B., Zhu X., Cai R., Yu Z., Guo W., Wang H., Dong Z., Lin M., Zhou X. and Zheng Y. (2021a). Circular RNA hsa_circ_0110389 promotes gastric cancer progression through upregulating SORT1 via sponging miR-127-5p and miR-136-5p. Cell Death Dis. 12, 639.

Liang Z., Zhao B., Hou J., Zheng J. and Xin G. (2021b). CircRNA circ-OGDH (hsa_circ_0003340) acts as a ceRNA to regulate glutamine metabolism and esophageal squamous cell carcinoma progression by the miR-615-5p/PDX1 axis. Cancer Manag. Res. 13, 3041-3053.

Liu Y.C., Li J.R., Sun C.H., Andrews E., Chao R.F., Lin F.M., Weng S.L., Hsu S.D., Huang C.C., Cheng C., Liu C.C. and Huang H.D. (2016). CircNet: a database of circular RNAs derived from transcriptome sequencing data. Nucleic Acids Res. 44, D209-215.

Liu L., Li Y., Zhang R., Li C., Xiong J. and Wei Y. (2020). MiR205HG acts as a ceRNA to expedite cell proliferation and progression in lung squamous cell carcinoma via targeting miR-299-3p/MAP3K2 axis. BMC Pulm. Med. 20, 163.

Liu Z., Lu X., Wen L., You C., Jin X. and Liu J. (2021). Hsa_circ_0014879 regulates the radiosensitivity of esophageal squamous cell carcinoma through miR-519-3p/CDC25A axis. Anticancer Drugs 33, e349-e361.

Lv X., Wang M., Qiang J. and Guo S. (2019). Circular RNA circ-PITX1 promotes the progression of glioblastoma by acting as a competing endogenous RNA to regulate miR-379-5p/MAP3K2 axis. Eur. J. Pharmacol. 863, 172643.

Panda A.C. (2018). Circular RNAs Act as miRNA sponges. Adv. Exp. Med. Biol. 1087, 67-79.

Paszek S., Gablo N., Barnas E., Szybka M., Morawiec J., Kolacinska A. and Zawlik I. (2017). Dysregulation of microRNAs in triple-negative breast cancer. Ginekol. Pol. 88, 530-536.

Samiei H., Sadighi-Moghaddam B., Mohammadi S., Gharavi A., Abdolmaleki S., Khosravi A., Kokhaei P., Bazzazi H. and Memarian A. (2019). Dysregulation of helper T lymphocytes in esophageal squamous cell carcinoma (ESCC) patients is highly associated with aberrant production of miR-21. Immunol. Res. 67, 212-222.

Smyth E.C., Lagergren J., Fitzgerald R.C., Lordick F., Shah M.A., Lagergren P. and Cunningham D. (2017). Oesophageal cancer. Nat. Rev. Dis. Primers. 3, 17048.

Su B., Cheng J., Yang J. and Guo Z. (2001). MEKK2 is required for T-cell receptor signals in JNK activation and interleukin-2 gene expression. J. Biol. Chem. 276, 14784-14790.

Wu C., Tong L., Wu C., Chen D., Chen J., Li Q., Jia F. and Huang Z. (2020). Two miRNA prognostic signatures of head and neck squamous cell carcinoma: A bioinformatic analysis based on the TCGA dataset. Cancer Med. 9, 2631-2642.

Xie Z.C., Li T.T., Gan B.L., Gao X., Gao L., Chen G. and Hu X.H. (2018). Investigation of miR-136-5p key target genes and pathways in lung squamous cell cancer based on TCGA database and bioinformatics analysis. Pathol. Res. Pract. 214, 644-654.

Yang S.M., Li S.Y., Hao-Bin Y., Lin-Yan X. and Sheng X. (2019). IL-11 activated by lnc-ATB promotes cell proliferation and invasion in esophageal squamous cell cancer. Biomed. Pharmacother. 114, 108835.

Yang B., Zang J., Yuan W., Jiang X. and Zhang F. (2021). The miR-136-5p/ROCK1 axis suppresses invasion and migration, and enhances cisplatin sensitivity in head and neck cancer cells. Exp. Ther. Med. 21, 317.

Yao J.T., Zhao S.H., Liu Q.P., Lv M.Q., Zhou D.X., Liao Z.J. and Nan K.J. (2017). Over-expression of CircRNA_100876 in non-small cell lung cancer and its prognostic value. Pathol. Res. Pract. 213, 453-456.

Zhang M. and Xin Y. (2018). Circular RNAs: a new frontier for cancer diagnosis and therapy. J. Hematol. Oncol. 11, 21.

Zhang X., Xu Y., Qian Z., Zheng W., Wu Q., Chen Y., Zhu G., Liu Y., Bian Z., Xu W., Zhang Y., Sun F., Pan Q., Wang J., Du L. and Yu Y. (2018a). circRNA_104075 stimulates YAP-dependent tumorigenesis

through the regulation of HNF4a and may serve as a diagnostic marker in hepatocellular carcinoma. Cell Death Dis. 9, 1091.

Zhang Y., Li C. and Chen M. (2018b). Prognostic value of immunohistochemical factors in esophageal small cell carcinoma (ESCC): analysis of clinicopathologic features of 73 patients. J. Thorac. Dis. 10, 4023-4031.

Zhang Q., Zhao X., Zhang C., Wang W., Li F., Liu D., Wu K., Zhu D., Liu S., Shen C., Yuan X., Zhang K., Yang Y., Zhang Y. and Zhao S. (2019). Overexpressed PKMYT1 promotes tumor progression and associates with poor survival in esophageal squamous cell carcinoma. Cancer Manag. Res. 11, 7813-7824.

Zhang X., Lu N., Wang L., Wang Y., Li M., Zhou Y., Yan H., Cui M., Zhang M. and Zhang L. (2020). Circular RNAs and esophageal cancer. Cancer Cell Int. 20, 362.

Zhou P.L., Wu Z., Zhang W., Xu M., Ren J., Zhang Q., Sun Z. and Han X. (2021a). Circular RNA hsa_circ_0000277 sequesters miR-4766-5p to upregulate LAMA1 and promote esophageal carcinoma progression. Cell Death Dis. 12, 676.

Zhou S., Guo Z., Zhou C., Zhang Y. and Wang S. (2021b). circ_NRIP1 is oncogenic in malignant development of esophageal squamous cell carcinoma (ESCC) via miR-595/SEMA4D axis and PI3K/AKT pathway. Cancer Cell Int. 21, 250.

Zhu J., Ye J., Zhang L., Xia L., Hu H., Jiang H., Wan Z., Sheng F., Ma Y., Li W., Qian J. and Luo C. (2017). Differential expression of circular RNAs in glioblastoma multiforme and its correlation with prognosis. Transl. Oncol. 10, 271-279.

Accepted December 1, 2022